Check for updates

AGU ADVANCING EARTH AND SPACE SCIENCES

Geophysical Research Letters

RESEARCH LETTER
10.1029/2025GL121190

Exploring Antarctic Feedback Mechanisms Using Two-Way Coupled Subglacial Hydrology and Ice Flow Modeling in the Siple Coast

Koi McArthur[1], Christine Dow[1,2], and Shivani Ehrenfeucht[2,3]

[1]Department of Applied Mathematics, University of Waterloo, Waterloo, ON, Canada, [2]Department of Geography and Environmental Management, University of Waterloo, Waterloo, ON, Canada, [3]Potsdam Institute for Climate Impact Research, Potsdam, Germany

Key Points:

- The modeled Siple Coast subglacial water system consists of low effective pressure, a dendritic channel system and subglacial lakes
- Thinning in the Siple Coast interior could lead to enhanced subglacial water storage and pulses in the motion of Ice Stream B
- Modeling with variable melt rates leads to a stabilizing feedback mechanism between ice motion and the subglacial hydrologic system

Supporting Information:

Supporting Information may be found in the online version of this article.

Correspondence to:

K. McArthur,
kr2mcart@uwaterloo.ca

Citation:

McArthur, K., Dow, C., & Ehrenfeucht, S. (2026). Exploring Antarctic feedback mechanisms using two-way coupled subglacial hydrology and ice flow modeling in the Siple Coast. *Geophysical Research Letters*, *53*, e2025GL121190. https://doi.org/10.1029/2025GL121190

Received 13 DEC 2025
Accepted 16 JUL 2026

Abstract The Siple Coast region of West Antarctica is known for its fast flowing, topographically unconstrained ice streams that evolve due to subglacial conditions. In this work, we analyze the nature of the Siple Coast subglacial hydrologic system and its interactions with the ice sheet using two-way coupled subglacial hydrology and ice flow modeling. Our modeling is consistent with observations of a water saturated till layer underlying the Siple Coast ice streams. We find that future thinning of ice upstream of Ice Stream B can lead to a hydraulic potential low that promotes water amalgamation and drainage through the ice stream, leading to pulses in ice motion. The inclusion of an ice-dynamics driven variable melt rate and the alteration of glacier driving stress due to subglacial lake geometry lead to stabilized motion of Ice Stream B. These feedbacks demonstrate the importance of coupled modeling for projecting the evolution of ice dynamics.

Plain Language Summary The Siple Coast, located in West Antarctica, has many subglacial lakes (pockets of accumulated water underneath glacier ice), and many regions of fast flowing ice that speed up and slow down as a result of processes underneath the ice sheet. For this work, we examine how the ice sheet interacts with its underlying water system by running numerical simulations that evolve both systems simultaneously over the Siple Coast. We additionally look to see how changes in meltwater production underneath the ice and the depth of subglacial lakes affect the ice sheet and vice versa, by incorporating these components into the simulations. We find that an area of ice that became thinner during the simulations triggered a flood in the water system underneath the ice sheet, that drained toward the ocean. As this flood passed underneath the ice sheet, it caused the ice to first speed up and then slow down over the period of roughly a decade. However, when variable meltwater production and subglacial lake depth are taken into account, lake depth and ice motion are more stable. The coupled interactions observed in this study highlight the importance of including evolving basal processes in ice flow modeling.

1. Introduction

The West Antarctic Ice Sheet (WAIS) has been a significant contributor to sea level rise over the past 20 years (Frederikse et al., 2020; Pritchard et al., 2009). Mass loss from WAIS has primarily been a result of ice dynamic processes in the Amundsen Sea Embayment (ASE), causing an increase of ice flux into the Southern Ocean. The Siple Coast region of WAIS, at present, is counteracting the ice loss in the ASE, with a net ice gain of 22.6 ± 1.9 Gt year^{-1} (Kim et al., 2024). The Siple Coast currently has four active ice streams, which shut down and reactivate on century-long timescales (Catania et al., 2012) due to internal ice sheet dynamics involving subglacial processes. The shutdown of the Kamb Ice Stream 170 years ago has been largely responsible for the recent trend of ice accumulation in the Siple Coast (Bougamont et al., 2015). However, the dynamic nature of the Siple Coast ice streams presents the possibility of future ice loss in the Siple Coast and warrants investigation into the region.

Antarctic subglacial hydrology has been shown to have a large impact on ice dynamics (C. F. Dow, 2022), with fast-flowing ice often corresponding to regions of low effective pressure (the difference between ice overburden pressure and subglacial water pressure). Underneath the Siple Coast ice streams, active subglacial lake drainage events have been found to result in ice acceleration (Siegfried et al., 2016; Stearns et al., 2008). The ice sheet also has the ability to shape the subglacial hydrologic system. Modeling studies have determined that ice geometry and basal traction can both impact the location where subglacial lakes form (Sergienko & Hulbe, 2011). When subglacial hydrologic processes are taken into account in ice sheet models they have been demonstrated to have a

© 2026 The Author(s). Geophysical Research Letters published by Wiley Periodicals LLC on behalf of American Geophysical Union.
This is an open access article under the terms of the Creative Commons Attribution-NonCommercial License, which permits use, distribution and reproduction in any medium, provided the original work is properly cited and is not used for commercial purposes.

19448007, 2026, 15, Downloaded from https://agupubs.onlinelibrary.wiley.com/doi/10.1029/2025GL121190 by Helmholtz-Zentrum Potsdam GFZ, Wiley Online Library on [29/10/2026]. See the Terms and Conditions (https://onlinelibrary.wiley.com/terms-and-conditions) on Wiley Online Library for rules of use; OA articles are governed by the applicable Creative Commons License

significant impact on sea level projections (Pelle et al., 2024; Zhao et al., 2025), highlighting the key role of such interactions.

Despite the important interplay between the subglacial hydrologic system and the ice sheet dynamics, current modeling studies at the catchment scale or larger are typically insufficient at capturing the feedback mechanisms between these two systems. Ice flow models at these scales are usually run without a subglacial hydrology model, or they are run coupled to a simple subglacial hydrology model such as in Bougamont et al. (2015). While such subglacial hydrology models are more computationally efficient, they lack key components of the subglacial hydrologic system, such as having both efficient and inefficient drainage. Only recently two-dimensional subglacial hydrology models with both inefficient and efficient drainage components such as the Glacier Drainage System (Werder et al., 2013, GlaDS) model and the Subglacial Hydrology and Kinetic Transient Interactions (A. Sommers et al., 2018, SHAKTI) model have been two-way coupled with ice flow models (Cook et al., 2022; Meyer et al., 2026; Pelle et al., 2024; A. N. Sommers et al., 2024). To date, only two of these two-way coupled models have been applied in Antarctica (Meyer et al., 2026; Pelle et al., 2024).

Here we investigate feedback mechanisms between the subglacial hydrologic system and the ice sheet, in the Siple Coast, using subglacial hydrology and ice flow modeling. The ice flow and subglacial hydrology models are run uncoupled and in a two-way coupled configuration to determine the impact of the coupling. Additionally, we test the importance of a temporally variable basal melt rate in the subglacial hydrologic system, and the importance of subglacial lakes altering the geometry of the ice sheet.

2. Methods

2.1. Overview

Our model domain consists of the Ross Ice Shelf and the Ross Sea subglacial hydrologic catchment (see Figure 1), calculated by assuming water is routed down the negative gradient of overburden hydraulic potential (sum of overburden pressure and elevation potential). The Transantarctic Mountains (TM) to the East of the Ross Ice Shelf are masked out of the model domain. We use the subglacial hydrology model GlaDS, with parameter choices given in Table S1 in Supporting Information S1, and discussed in Text S7 in Supporting Information S1. To model ice flow, we use the Shallow Shelf Approximation (MacAyeal, 1989, SSA) of Stokes flow for stress balance, and we use the mass transport model described in Larour et al. (2012). These models are implemented in the Ice-sheet and Sea-level System Model (Larour et al., 2012, ISSM). Details on the application of these models are discussed in Texts S1 and S2 in Supporting Information S1, information about the computational mesh is given in Text S3 in Supporting Information S1, and boundary conditions are given in Text S4 in Supporting Information S1.

2.2. Simulations

A schematic of the simulations and their properties is given in Figure 1g. We run a 100 years steady-state subglacial hydrology simulation with constant ice velocity from MEaSUREs v2 (Rignot et al., 2017) and ice geometry from BedMachine Antarctica v3.4 (Morlighem et al., 2020) using GlaDS (Model-H), and seven transient ice flow or coupled simulations from 2010 to 2100 with various model modifications and surface mass balance (SMB) forcing scenarios. Two of these are ice flow-only simulations that take effective pressure from the final timestep of Model-H, while the other five simulations use coupled subglacial hydrology and ice flow. The models are set up to test the impact of SMB forcing (Model-I vs. Model-I-control and Model-C vs. Model-C-control), variable effective pressure (ice-flow vs. coupled models), subglacial lakes uplifting the glacier and altering driving stress (Model-C vs. Model-CD and Model-CM vs. Model-CF), and temporally-variable basal melt inputs driven by changes in ice-flow speed (Model-C vs. Model-CM and Model-CD vs. Model-CF). To initialize these transient simulations, we use inverse methods (Morlighem et al., 2013) and a model relaxation procedure that aims to approximate the conditions of the ice sheet in 2010, described in Text S6 in Supporting Information S1. They are forced with SMB from either an SSP5-8.5 forcing scenario (Kittel, 2021; Kittel et al., 2021), or the mean SMB from 1980 to 2010 (Kittel, 2021; Kittel et al., 2021). Basal mass balance over the floating portion of the domain is taken from Adusumilli et al. (2020), and in the uncoupled simulations, basal mass balance over the grounded portion of the domain is taken from the initMIP-Antarctica control run final time step (Seroussi et al., 2019). The grounding line is allowed to evolve with the ice geometry, and the floating ice front is fixed.

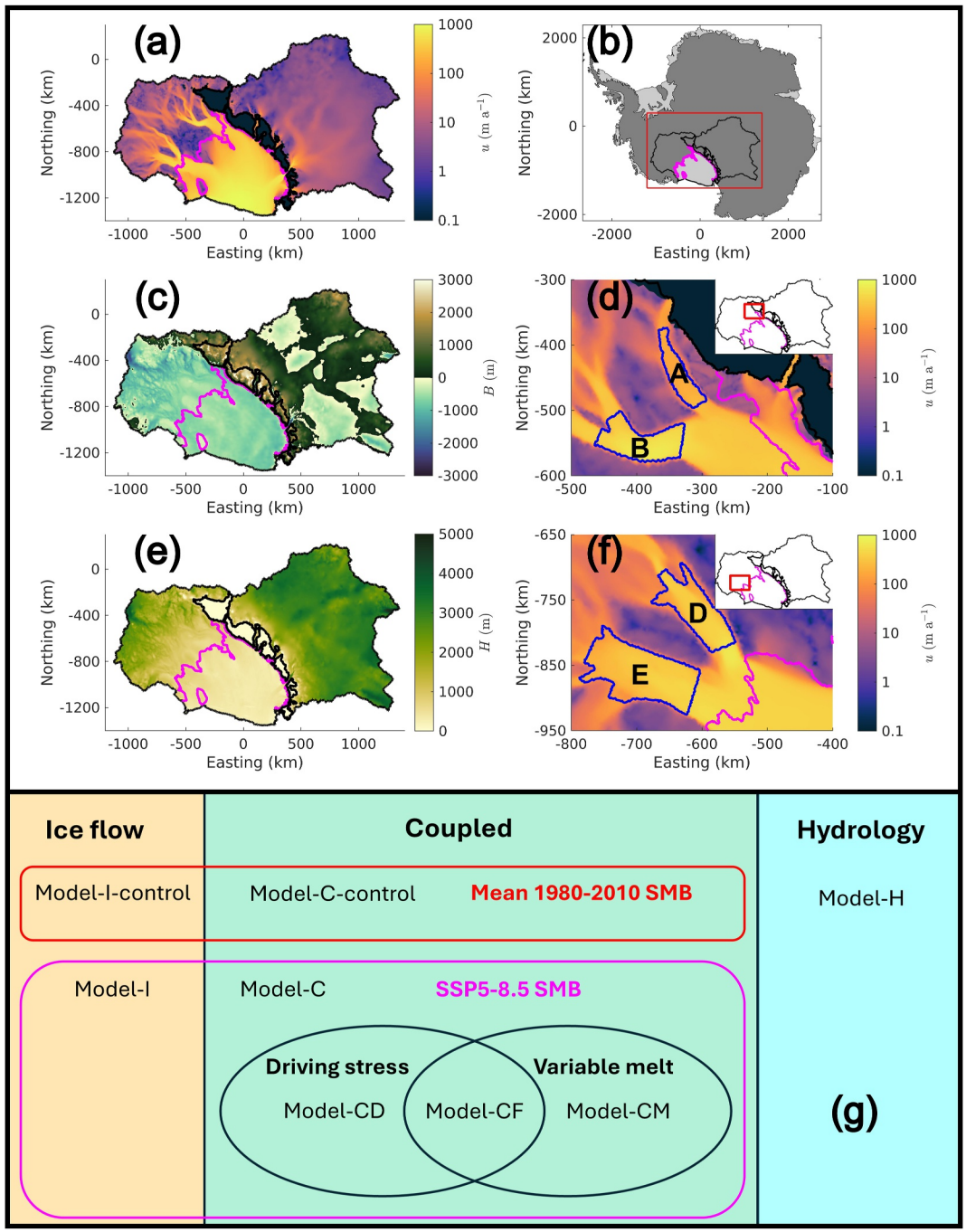


Figure 1. (a) Model domain in relation to the AIS outlined in black with the grounding line in pink, the Transantarctic Mountains shaded in black, and the axes of (b–d) in red. (b) Bed topography (m) and (c) ice thickness (m) from BedMachine Antarctica v3.4 (Morlighem et al., 2020). (d–f) ice speed (m year^{-1}) from MEaSUREs v2 (Rignot et al., 2017). Zoomed in view of (e) ice stream A/B and (f) ice stream D/E with ice streams outlined in blue and inset maps of plot axes in relation to the model domain in red. (g) Schematic of simulations and their properties, "Driving stress" refers to subglacial lake geometry altering glacier driving stress.

2.3. Coupling

The coupled models pass effective pressure from GlaDS into the friction law in the SSA equations, ice velocity from the stress balance model into GlaDS and the mass transport model, and ice geometry from the mass transport model into GlaDS and the stress balance model. We use a regularized Coulomb friction law based on

19448007, 2026, 15, Downloaded from https://agupubs.onlinelibrary.wiley.com/doi/10.1029/2025GL121190 by Helmholtz-Zentrum Potsdam GFZ, Wiley Online Library on [29/10/2026]. See the Terms and Conditions (https://onlinelibrary.wiley.com/terms-and-conditions) on Wiley Online Library for rules of use; OA articles are governed by the applicable Creative Commons License

19448007, 2026, 15, Downloaded from https://agupubs.onlinelibrary.wiley.com/doi/10.1029/2025GL121190 by Helmholtz-Zentrum Potsdam GFZ, Wiley Online Library on [29/10/2026]. See the Terms and Conditions (https://onlinelibrary.wiley.com/terms-and-conditions) on Wiley Online Library for rules of use; OA articles are governed by the applicable Creative Commons License

Schoof (2005) and Gagliardini et al. (2007), but modified so that the response of the basal shear stress to changes in effective pressure and ice motion is dependent on subglacial conditions predicted from GlaDS (Text S5 in Supporting Information S1).

Some of the coupled simulations also incorporate the impact of subglacial lakes lifting up the ice sheet by including subglacial lake geometry in the calculation of the driving stress of the stress balance equations (Text S2 in Supporting Information S1). In these simulations the ice surface is assumed to be instantaneously uplifted by an amount equal to the subglacial lake depth, which alters ice surface gradients and glacier driving stress.

The coupled simulations either take basal mass balance over the grounded domain from the initMIP-Antarctica control run final time step (Seroussi et al., 2019), which is temporally static but spatially variable, or calculate it from a combination of melt from geothermal heat flux (Stål et al., 2020, 2021) and frictional heating of ice, which evolves with the basal shear stress and is therefore both spatially and temporally variable (Text S2 in Supporting Information S1).

A flowchart of the model coupling with the inclusion of subglacial lake geometry in the driving stress and using a temporally variable basal melt input is given in Figure S1 in Supporting Information S1.

3. Results

3.1. Subglacial Hydrology

In Model-H, much of the Ross Sea subglacial hydrologic catchment (92.1%) has a fraction of flotation (ratio of subglacial water pressure to ice overburden pressure) greater than 0.8 (Figure 2a). These values are elevated within the Siple Coast ice streams and Byrd trough, where the fraction of flotation is often above 0.95 (29.4% of the total grounded domain). Sometimes flotation is reached in regions where there are subglacial lakes (0.0379% of the total grounded domain). Between the Siple Coast ice streams lie isolated patches of high effective pressure (low fraction of flotation), which correspond to ice rises where the glacier bed and the ice surface lie hundreds of meters above the surrounding topography, creating hydraulic potential highs. The fraction of flotation surrounding the TM is generally low except in the troughs that feed water into the ocean. East of the TM the fraction of flotation is generally high, as water is pressurized underneath thick ice in the interior of East Antarctica.

Subglacial channels form underneath the ice streams of the Siple Coast, including under the stagnated Kamb Ice Stream, and the outlet glaciers running through the TM (Figure 2b). Although the channels running through the TM have a clear discharge path, this is less evident in the Siple Coast ice streams where channels form as a result of low effective pressure and low channel closing rates. The tortuous nature of the Siple Coast channel system can be attributed to the relatively flat ice surface creating small gradients in hydraulic potential. Subglacial lakes form in the Byrd trough and underneath Ice Streams B, D, and E (Figure 2c). The hydrology sheet thickness reaches close to the typical bedrock bump height (8 cm) underneath the ice streams of the Siple Coast, upglacier of Ice Stream B, and in Byrd trough (Figure 2d). A thinner hydrology sheet exists outside of these areas, quickly falling to zero near the TM and the Siple Coast ice rises where the subglacial hydrologic system appears to be inactive.

The subglacial lakes of the Siple Coast first form higher up in the ice streams, away from the grounding line, and drain forming a chain of subglacial lakes, which eventually reach near steady state, with no major changes in lake depth after 60 years. Although these lakes reach depths of up to 50 m earlier in the model run (Figure 2e), this could be a consequence of a still developing hydrologic system. Lake thickness near the end of the model run, which is substantially smaller (less than 15 m), should be taken as typical modeled lake depth in these areas.

3.2. Ice Flow

Both ice flow models (Model-I, and Model-I-control) follow the same general patterns over the 90 years simulation (Figures 3a–3d). All Siple Coast ice streams slow down over the course of the simulation. In Model-I, Ice Stream A slows by 70.2 m year^{-1}, Ice Stream B by 26.2 m year^{-1}, and ice streams D and E by 7.08 m year^{-1} and 6.13 m year^{-1}, respectively. Ice stream speeds are calculated from the areal average of ice speed in the ice stream locations outlined in Figures 1d and 1e. Ice Streams A and B thin, and the Kamb Ice Stream thickens throughout the simulation, while the ice thickness of Ice Streams D and E remains nearly constant. The ice upglacier of the TM and in the troughs running through the TM thicken in some places in excess of 40 m. Notably in this area, the ice upglacier of the Byrd trough thickens in excess of 50 m, and speeds up by more than 100 m

10.1029/2025GL121190

19448007, 2026, 15, Downloaded from https://agupubs.onlinelibrary.wiley.com/doi/10.1029/2025GL121190 by Helmholtz-Zentrum Potsdam GFZ, Wiley Online Library on [29/10/2026]. See the Terms and Conditions (https://onlinelibrary.wiley.com/terms-and-conditions) on Wiley Online Library for rules of use; OA articles are governed by the applicable Creative Commons License

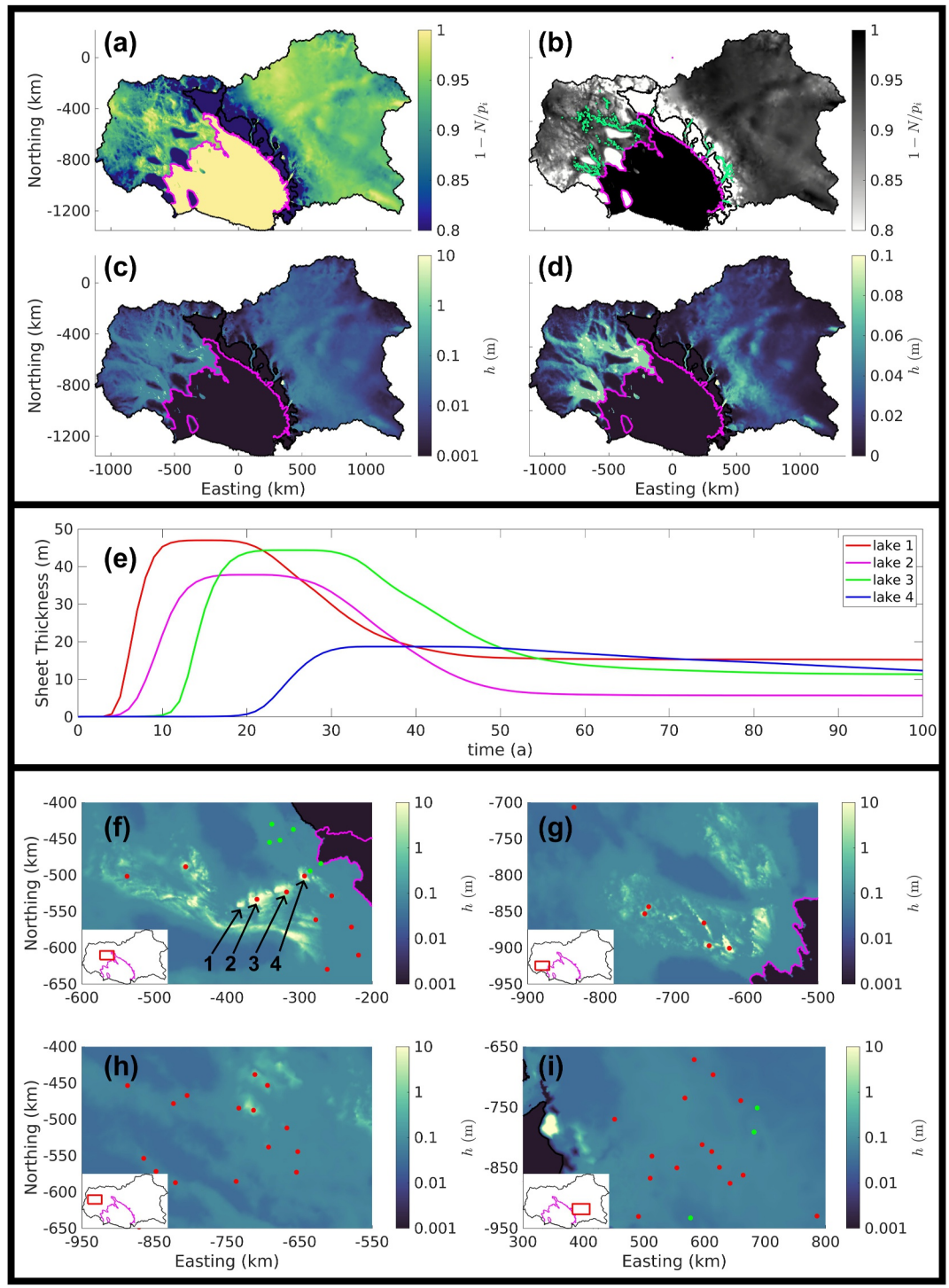


Figure 2. (a) and (b) Flotation fraction from the final timestep of Model-H with channels with discharge larger than 1 $m^3\ s^{-1}$ in green in (b). (c) and (d) hydrology sheet thickness (m) from the final timestep of Model-H, (c) has a log scale to better visualize subglacial lake locations. (e) A timeseries plot of subglacial lake depths (m), with lake locations shown in (f), labeled as 1, 2, 3, and 4. (f–i) maximum hydrology sheet thickness (m) over the course of Model-H with dots representing lakes from Livingstone et al. (2022) (red for active, green for stable), and inset maps with plot axes in relation to the model domain in red. (f–i) are zoomed in on the (f) ice stream A/B region, (g) ice stream D/E region, (h) upglacier of Ice Stream B, (i) upglacier of Byrd Glacier. Pink lines represent the grounding line and black lines represent the domain boundary in the spatial plots.

10.1029/2025GL121190

19448007, 2026, 15, Downloaded from https://agupubs.onlinelibrary.wiley.com/doi/10.1029/2025GL121190 by Helmholtz-Zentrum Potsdam GFZ, Wiley Online Library on [29/10/2026]. See the Terms and Conditions (https://onlinelibrary.wiley.com/terms-and-conditions) on Wiley Online Library for rules of use; OA articles are governed by the applicable Creative Commons License

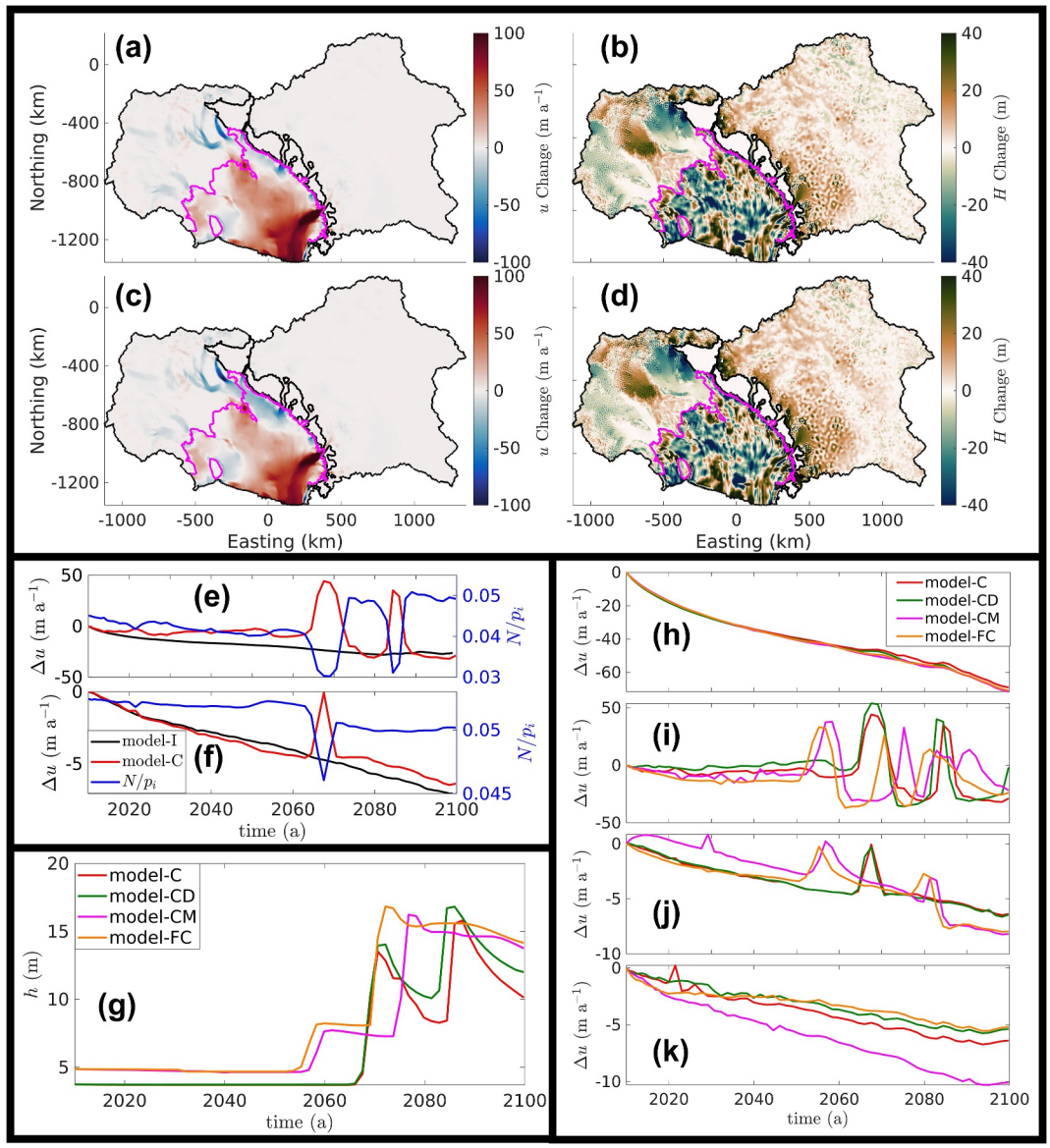


Figure 3. Ice flow and coupled results, including (a) change in ice speed (m year^{-1}) in Model-I, (b) change in ice thickness (m) in Model-I, (c) change in ice speed (m year^{-1}) in Model-I-control, and (d) change in ice thickness (m) in Model-I-control. (e) and (f) changes in ice speed (m year^{-1}) and effective pressure for Ice Streams B and D respectively in Model-I and Model-C. (g) A timeseries of the lake depths (m) of Lake 2 from Figure 2f in the coupled models. (h–k) timeseries of ice speed (m year^{-1}) in the Siple Coast ice streams (Figures 1d and 1f) from the coupled models, (h) Ice Stream A, (i) Ice Stream B, (j) Ice Stream D, and (k) Ice Stream E. Pink lines represent the initial grounding line and black lines represent the domain boundary in the spatial plots.

year^{-1} downstream of the grounding line as a result of poorly constrained ice rigidity and friction (Figure 3b). The pockmark pattern of ice thickness change upglacier of the TM could be a model-grid artifact. SMB forcing has little effect on ice dynamics, except during the last 18 years of the simulation in Ice Stream A, which slows more rapidly, and Ice Stream B, which ceases deceleration (Figures 3a–3d).

3.3. Coupled Interactions

The coupled models and the ice flow-only models have similar trends of ice motion for Ice Streams A and E throughout the simulation, with more ice speed variability in the coupled models as a result of the influence from the subglacial hydrologic system. However, the ice motion trends for Ice Streams B and D diverge significantly

19448007, 2026, 15, Downloaded from https://agupubs.onlinelibrary.wiley.com/doi/10.1029/2025GL121190 by Helmholtz-Zentrum Potsdam GFZ, Wiley Online Library on [29/10/2026]. See the Terms and Conditions (https://onlinelibrary.wiley.com/terms-and-conditions) on Wiley Online Library for rules of use; OA articles are governed by the applicable Creative Commons License

between the coupled models and the ice flow-only models (Figures 3e and 3f). Ice Stream B has two periods of significant ice acceleration followed quickly by ice deceleration (pulses in ice motion) in Model-C. During the first pulse, ice increases in speed by 52.2 m year^{-1} before decreasing by 75.0 m year^{-1} (Figure 3e). Ice Stream D has one such ice pulse event, though on a much smaller scale (an increase of 4.54 m year^{-1} and a decrease of 4.45 m year^{-1}; Figure 3f). In the case of Ice Stream B, these events coincide with flooding of the subglacial hydrologic system (many elements with hydrology sheet thickness above the typical bedrock bump height) upglacier of Ice Stream B and the drainage of this water build-up through Ice Stream B to the grounding line. We find ice speed to have a high negative correlation with effective pressure (correlation coefficient of −0.942), further indicating that these pulses in ice motion are driven by changes in the subglacial hydrologic system.

The coupled models with a variable melt rate (Model-CM and Model-CF) have three pulses in ice motion in Ice Stream B compared to two in the coupled models with constant melt (Model-C and Model-CD, Figure 3i). The pulses in ice motion occur at different times in Model-CM and Model-CF compared to Model-C and Model-CD, with the prior two models having a first pulse that occurs earlier in the simulation than the latter two models. Model-CM has enhanced ice speed variability (small year to year changes in ice motion, rather than the pulses in ice motion) in Ice Stream B compared to Model-C, and Model-CF has the smallest variability in ice speed in all the Siple Coast ice streams (Figures 3h–3k). Compared to Model-C, the inclusion of subglacial lake depth in the driving stress calculation in Model-CD leads to an additional slowdown of 14.6 m year^{-1} at the end of the first pulse in ice motion (Figure 3i). An enhanced slowdown is not visible in Model-CF compared to Model-CM. However, both Model-CD and Model-CF have deeper lakes than Model-C and Model-CM respectively (Figure 3g).

4. Discussion

In both ice flow models, Ice Stream B decelerates from 2010 to 2082 where its ice speed levels out in Model-I. The initial rate of deceleration (over the first 10 years of the simulation) is 1.04 m year^{-2}, which is low compared to Stearns et al. (2005), who observed the ice dynamics of Ice Stream B from 1987 to 1997 using interferometric satellite radar (InSAR), and found a slowdown of 2.9–4.1 m year^{-2}. Ice Stream B only slows in the coupled models after the drainage of subglacial lakes, suggesting a possible over-representation of subglacial hydrologic influence in the friction law of the coupled models. Catania et al. (2012) noted that the rate of deceleration observed by Stearns et al. (2005) would result in the complete stagnation of Ice Stream B by 2070–2080. Bougamont et al. (2015) modeled the ice dynamics of the Siple Coast 250 years into the future and also found a slowdown of Ice Stream B, which did not stagnate or speed up over the course of their 250 years simulation. A similar prolonged slowdown is observed in Model-I-control, which like the model in Bougamont et al. (2015), doesn't use a SMB forcing scenario. This highlights the potential importance of future SMB forcing in the region. Catania et al. (2012) and Bougamont et al. (2015) both suggested that the Kamb Ice Stream will reactivate following the slow down, followed by a possible stagnation of Ice Stream B. Bougamont et al. (2015) found that the Kamb Ice Stream reactivation occurred 100 years into their model run, suggesting that a Kamb Ice Stream reactivation may not be expected in the 90 years simulations of this study. Indeed, no such reactivation is observed in any of our models.

In all coupled models, there is significant flooding upglacier of Ice Stream B, which drains toward the grounding line. This flooding is a consequence of the gradual ice thinning upglacier of Ice Stream B, which decreases hydraulic potential in an area where subglacial water pressure is already very close to ice overburden pressure (Figure 2a). Once ice overburden pressure is reached, the hydrology sheet thickness increases rapidly, resulting in flooding of the subglacial hydrologic system. This flooding results in pulses of ice motion on scales of decades (Figure 3i). The amplitude of these pulses of ice motion is found to be largely dependent on the choice of ζ, a parameter in the friction law of the ice flow model (Text S5 in Supporting Information S1). A larger ζ means that the basal shear stress responds more strongly to changes in effective pressure/hydraulic potential. Due to the sensitivity of ice motion on the choice of ζ, it is difficult to quantify the impact of the ice thinning upglacier of Ice Stream B. However, it is clear that if such thinning occurs, it would result in enhanced water storage capacity and associated ice speedup events. A future study comparing modeled and observed transient velocity patterns could be a way to help constrain the value of ζ.

A temporally variable melt rate is found to have a large impact on coupled dynamics, with additional ice pulses in Ice Stream B and D in Model-CM and Model-CF (Figures 3i and 3k). This is likely due to the generally lower

19448007, 2026, 15, Downloaded from https://agupubs.onlinelibrary.wiley.com/doi/10.1029/2025GL121190 by Helmholtz-Zentrum Potsdam GFZ, Wiley Online Library on [29/10/2026]. See the Terms and Conditions (https://onlinelibrary.wiley.com/terms-and-conditions) on Wiley Online Library for rules of use; OA articles are governed by the applicable Creative Commons License

effective pressures of the variable melt simulations, which have larger inputs of meltwater due to the temperate bed assumption requiring all geothermal heat flux go toward melting basal ice. The temporally constant melt rate was calculated from the initMIP Antarctica ISSM control run, which in comparison, used a thermomechanical model, which would not estimate basal melt in cold regions of the bed. In addition to these extra ice pulses explained by lower effective pressure, variable melt is found to have a destabilizing effect on the motion of ice streams (small year to year perturbations in ice motion, rather than large pulses in ice motion). However, when ζ is increased, a stabilizing effect on the motion of ice streams is observed (Text S5 in Supporting Information S1). For a sufficiently large ζ, increases in basal shear stress will result in enhanced meltwater production, which will lower the effective pressure, reducing basal shear stress. This negative feedback loop acts to stabilize basal shear stress and hence, ice motion. However, when ζ is sufficiently small, the change in effective pressure will have little impact on the basal shear stress, so there will be no stabilizing effect on ice motion. The increased ice speed variability in Model-CM compared to Model-C can be attributed to an effective pressure that is lower in Model-CM, causing larger perturbations in the basal shear stress, but not low enough to trigger the negative feedback mechanism that stabilizes ice motion. Given the melt related feedback mechanisms observed in this study, future work could couple a thermal/enthalpy model to the subglacial hydrology and ice flow models to better understand these feedback mechanisms.

Model-CF features more ice speed and lake depth stability than Model-CM, particularly in Ice Stream B, where there is an extra increase in ice speed in Model-CM in 2087 (Figures 3g–3k). In Model-CF, when lake depth increases it lowers driving stress, which slows down the ice stream, consequently reducing basal meltwater production and draining the subglacial lake. This negative feedback mechanism is exclusive to Model-CF, as it requires both a variable melt rate and an ice geometry response to changes in lake depth. The impact of these additional coupling components on subglacial lake depth and ice motion shows the importance of including these mechanisms in two-way coupled modeling moving forward.

Channels form in the Siple Coast ice streams and in the outlet glaciers of the TM (Figure 2b). Channels underneath the Siple Coast ice streams don't follow a main discharge path, with channels of comparable discharge forming on element edges close to each other but flowing in different directions. The low ice surface slopes of the Siple Coast, which generate small hydraulic potential gradients, may be in part responsible for this tortuous channel system. Carter et al. (2017) modeled subglacial lake drainage and determined that for fill/drain cycles to occur on timescales associated with Siple Coast subglacial lakes—a couple of years—channels incised into sediment (sediment canals) instead of ice (R-channels) are needed. Underlying the Siple Coast ice streams is a soft till layer (Blankenship et al., 1986; Engelhardt et al., 1990), which could conceivably allow for the growth of such sediment canals. GlaDS assumes a hard glacier bed and the formation of R-channels as opposed to sediment canals; assumptions that are inaccurate under the Siple Coast ice streams. However, given the distributed nature of the sheet system in GlaDS, it has been argued that GlaDS could apply to soft glacier beds (Werder et al., 2013). Therefore, the modeled large hydrology sheet thickness and tortuous channel system under the Siple Coast ice streams could suggest the existence of a water saturated till layer and sediment canals. Future work with soft-bed specific subglacial hydrology models (Kazmierczak et al., 2024; Minchew & Meyer, 2020; Warburton et al., 2023) may be necessary to better model subglacial conditions of the Siple Coast.

4.1. Subglacial Lakes

Subglacial lakes form in all models where GlaDS is run, primarily underneath ice streams B, D, and E, and underneath Byrd Glacier. Lakes do not form under Ice Stream A or the Kamb Ice Stream in any model, and lakes only form in the interior of the East Antarctic Ice Sheet in Model-CM and Model-CF, where there is sufficient meltwater in the subglacial hydrological system. Comparing against known locations of subglacial lakes from Livingstone et al. (2022), we find both lakes from Livingstone et al. (2022) that do not appear in our models, and lakes in our models that do not appear in Livingstone et al. (2022). Lakes that appear in both our models and Livingstone et al. (2022) lie underneath ice streams B and E in the Siple Coast (Figures 2f and 2g). Livingstone et al. (2022) found lakes under Ice Stream A (Figure 2f) and the Kamb Ice Stream (Kim et al., 2016), which do not appear in our models, and our models suggest the existence of lakes under Ice Stream D (Figure 2g), which were not observed by Livingstone et al. (2022).

The discrepancy between known and modeled subglacial lake locations could be a consequence of ice geometry and bed topography inputs from Morlighem et al. (2020). Lakes occur in regions where there are hydraulic

19448007, 2026, 15, Downloaded from https://agupubs.onlinelibrary.wiley.com/doi/10.1029/2025GL121190 by Helmholtz-Zentrum Potsdam GFZ, Wiley Online Library on [29/10/2026]. See the Terms and Conditions (https://onlinelibrary.wiley.com/terms-and-conditions) on Wiley Online Library for rules of use; OA articles are governed by the applicable Creative Commons License

potential lows, which are dependent on ice surface and bed elevation gradients. The bed topography data from Morlighem et al. (2020) was created using observed ice speed and thickness data, and applying mass conservation to interpolate the data over the ice sheet. The bed elevation derived from this process does not account for the existence of large layers of subglacial water and assumes the glacier bed to be located where the surface of a hypothetical subglacial lake may be. This method likely overestimates the bed elevation in regions with subglacial lakes, and can potentially eliminate the hydraulic potential lows required for these lakes to form in GlaDS. Therefore, stable lakes identified by Livingstone et al. (2022)—lakes that have approximately equal inflow and outflow—may not be observed in our models due to an overestimation of bed elevation. Active lakes that have a maximum lake depth at the time of surface elevation observation will also overestimate bed elevation and may not appear in our models. Additionally, the nature of using mass conservation and sparse ice thickness measurements to determine bed topography results in both ice thickness and bed elevation errors, to which subglacial lake locations are highly sensitive. The absence of observed lakes in our models is therefore expected, but modeled lakes that are yet to be observed may still exist, and warrant inspection.

Lakes in GlaDS reach steady state when the effective pressure equals zero. For subglacial lakes, the effective pressure is a function of the hydrology sheet thickness and the hydraulic potential. Therefore, the evolution of lake depth is controlled by the evolution of the hydraulic potential field, which in GlaDS often changes on spatial scales larger than the width of the subglacial lake. This can cause multiple lakes to fill and drain simultaneously, where in reality, upstream lakes may drain into downstream lakes, as observed by Siegfried et al. (2016), downstream of ice streams A and B in the Whillans Ice Plain. In Model-H the drainage of lakes further upstream in Ice Stream B is not required for the lakes further downstream to fill (Figure 2e).

The inclusion of subglacial lake geometry in the calculation of the driving stress in the SSA generally led to deeper lakes and larger drops in ice stream speed at the tail end of pulses in ice motion (Figures 3g and 3i). Given that the ice surface slope typically plays a larger role in subglacial water routing than the bed slope (Shreve, 1972), subglacial lakes will typically form in regions with a depressed ice surface, and increasing subglacial lake depth will typically decrease driving stress. In Model-CD the ice speed drops almost 15 m year^{-1} more after the first ice pulse in Ice Stream B compared to Model-C (Figure 3i), corresponding to lower driving stresses due to increased lake depths. The generally deeper lakes in Model-CD and Model-CF are a consequence of continually thinning ice creating more substantial hydraulic potential lows as the lakes fill.

The implementation of subglacial lakes used in this study relies on a localized viscous creep mechanism and changes in the hydraulic potential field to drive lake evolution. In reality, subglacial lakes should trigger a non-local visco-elastic response from the ice sheet, which drives the evolution of the hydraulic potential field. Such a response would require a non-local evolution of the hydrology sheet thickness, increasing computational expense and potential difficulty of coupling. Future work on improving the implementation of subglacial lakes could include a visco-elastic response from the ice sheet, or an improved parameterization of the hydrology sheet opening rate.

5. Conclusions

The Siple Coast region of West Antarctica has long been an area of interest in the glaciological community due to its fast flowing topographically unconstrained ice streams that evolve on timescales of hundreds of years. We investigated feedback mechanisms between the subglacial hydrological system and the ice sheet through two-way coupled subglacial hydrology and ice flow modeling, with the inclusion of subglacial lake geometry in the driving stress calculation and a temporally variable melt rate due to geothermal heat flux and frictional melting of ice. We found that thinning of the region upglacier of Ice Stream B can lead to an enhanced hydraulic potential low, which may result in flooding of the subglacial hydrologic system, which drains toward the grounding line, causing multi-decadal pulses in the motion of Ice Stream B. A temporally variable melt rate was found to stabilize ice motion for a sufficiently large coupling strength constant, as a result of a negative feedback mechanism between the basal shear stress and ice speed. When a variable melt rate and the inclusion of subglacial lake geometry in the driving stress calculation were applied together, an additional negative feedback mechanism that stabilizes lake depth, and ice stream motion was identified. These feedback mechanisms highlight the importance of applying coupled hydrology and ice dynamics models for Antarctic Ice Sheet projections, including features such as temporally-variable melt inputs and lake geometry.

Conflict of Interest

The authors declare no conflicts of interest relevant to this study.

Availability Statement

We use version 4.24 of the open-source ISSM software, available from https://github.com/ISSMteam/ISSM. We use ice velocity from MEaSUREs v2 (Rignot et al., 2017), ice geometry from BedMachine Antarctica v3.4 (Morlighem et al., 2020), geothermal heat flux from Stål et al. (2020), surface mass balance from Kittel et al. (2021), ice shelf melt rates from Adusumilli et al. (2020), grounded basal melt rates from the initMIP Antarctica ISSM Control run final time step (Seroussi et al., 2019), and atmospheric temperature from RACMO v2.3 (van Wessem et al., 2023). Model outputs for plotting are available at McArthur et al. (2026).

Acknowledgments

K. McArthur was supported by the Natural Sciences and Engineering Research Council of Canada (NSERC), Canada Graduate Scholarship, and the Ontario Graduate Scholarship. C. Dow and S. Ehrenfeucht were supported by NSERC (NSERC RGPIN-03761-2017), and C. Dow received additional funding from the Canada Research Chairs Program (CRC 950-231237). The authors would like to thank the Digital Research Alliance of Canada for access to supercomputing resources.

References

Adusumilli, S., Fricker, H. A., Medley, B., Padman, L., & Siegfried, M. (2020). Interannual variations in meltwater input to the Southern Ocean from Antarctic ice shelves. *Nature Geoscience*, *13*(9), 616–620. https://doi.org/10.1038/s41561-020-0616-z

Blankenship, D. D., Bentley, C. R., Rooney, S. T., & Alley, R. B. (1986). Seismic measurements reveal a saturated porous layer beneath an active Antarctic ice stream. *Nature*, *322*(6074), 54–57. https://doi.org/10.1038/322054a0

Bougamont, M., Christoffersen, P., Price, S. F., Fricker, H. A., Tulaczyk, S., & Carter, S. P. (2015). Reactivation of Kamb Ice Stream tributaries triggers century-scale reorganization of Siple Coast ice flow in West Antarctica. *Geophysical Research Letters*, *42*(20), 8471–8480. https://doi.org/10.1002/2015GL065782

Carter, S. P., Fricker, H. A., & Siegfried, M. R. (2017). Antarctic subglacial lakes drain through sediment-floored canals: Theory and model testing on real and idealized domains. *The Cryosphere*, *11*(1), 381–405. https://doi.org/10.5194/tc-11-381-2017

Catania, G., Hulbe, C., Conway, H., Scambos, T., & Raymond, C. (2012). Variability in the mass flux of the Ross ice streams, West Antarctica, over the last millennium. *Journal of Glaciology*, *58*(210), 741–752. https://doi.org/10.3189/2012JoG11J219

Cook, S. J., Christoffersen, P., & Todd, J. (2022). A fully-coupled 3D model of a large Greenlandic outlet glacier with evolving subglacial hydrology, frontal plume melting and calving. *Journal of Glaciology*, *68*(269), 486–502. https://doi.org/10.1017/jog.2021.109

Dow, C. F. (2022). The role of subglacial hydrology in Antarctic ice sheet dynamics and stability: A modelling perspective. *Annals of Glaciology*, *63*(87–89), 49–54. https://doi.org/10.1017/aog.2023.9

Engelhardt, H., Humphrey, N., Kamb, B., & Fahnestock, M. (1990). Physical conditions at the base of a fast moving Antarctic ice stream. *Science*, *248*(4951), 57–59. https://doi.org/10.1126/science.248.4951.57

Frederikse, T., Landerer, F., Caron, L., Adhikari, S., Parkes, D., Humphrey, V. W., et al. (2020). The causes of sea-level rise since 1900. *Nature (London)*, *584*(7821), 393–397. https://doi.org/10.1038/s41586-020-2591-3

Gagliardini, O., Cohen, D., Råback, P., & Zwinger, T. (2007). Finite-element modeling of subglacial cavities and related friction law. *Journal of Geophysical Research*, *112*(F2), F02027. https://doi.org/10.1029/2006jf000576

Kazmierczak, E., Gregov, T., Coulon, V., & Pattyn, F. (2024). A fast and simplified subglacial hydrological model for the Antarctic Ice Sheet and outlet glaciers. *The Cryosphere*, *18*(12), 5887–5911. https://doi.org/10.5194/tc-18-5887-2024

Kim, B.-H., Lee, C.-K., Seo, K.-W., Lee, W. S., & Scambos, T. (2016). Active subglacial lakes and channelized water flow beneath the Kamb Ice Stream. *The Cryosphere*, *10*(6), 2971–2980. https://doi.org/10.5194/tc-10-2971-2016

Kim, B.-H., Seo, K.-W., Lee, C.-K., Kim, J.-S., Lee, W. S., Jin, E. K., & van den Broeke, M. (2024). Partitioning the drivers of Antarctic glacier mass balance (2003–2020) using satellite observations and a regional climate model. *Proceedings of the National Academy of Sciences - PNAS*, *121*(41), e2322622121-. https://doi.org/10.1073/pnas.2322622121

Kittel, C. (2021). The cryosphere: MAR and ESMs data [Dataset]. *Zenodo*. https://doi.org/10.5281/zenodo.4459259

Kittel, C., Amory, C., Agosta, C., Jourdain, N. C., Hofer, S., Delhasse, A., et al. (2021). Diverging future surface mass balance between the Antarctic ice shelves and grounded ice sheet. *The Cryosphere*, *15*(3), 1215–1236. https://doi.org/10.5194/tc-15-1215-2021

Larour, E., Seroussi, H., Morlighem, M., & Rignot, E. (2012). Continental scale, high order, high spatial resolution, ice sheet modeling using the Ice Sheet System Model (ISSM). *Journal of Geophysical Research*, *117*(F1), F01022. https://doi.org/10.1029/2011JF002140

Livingstone, S. J., Li, Y., Rutishauser, A., Sanderson, R. J., Winter, K., Mikucki, J. A., et al. (2022). Subglacial lakes and their changing role in a warming climate. *Nature Reviews Earth & Environment*, *3*(2), 106–124. https://doi.org/10.1038/s43017-021-00246-9

MacAyeal, D. R. (1989). Large-scale ice flow over a viscous basal sediment: Theory and application to ice stream B, Antarctica. *Journal of Geophysical Research*, *94*(B4), 4071–4087. https://doi.org/10.1029/jb094ib04p04071

McArthur, K., Dow, C., & Ehrenfeucht, S. (2026). Data for "Exploring Antarctic feedback mechanisms using two-way coupled subglacial hydrology and ice flow modeling in the Siple Coast [Dataset]. *Zenodo*. https://doi.org/10.5281/zenodo.19555986

Meyer, C. R., Warburton, K. L. P., Sommers, A. N., & Minchew, B. M. (2026). A model of water extraction from the subglacial hydrologic system under idealized conditions. *The Cryosphere*, *20*(5), 2659–2680. https://doi.org/10.5194/tc-20-2659-2026

Minchew, B. M., & Meyer, C. R. (2020). Dilation of subglacial sediment governs incipient surge motion in glaciers with deformable beds. *Proceedings of the Royal Society A: Mathematical, Physical & Engineering Sciences*, *476*(2238), 20200033. https://doi.org/10.1098/rspa.2020.0033

Morlighem, M., Rignot, E., Binder, T., Blankenship, D., Drews, R., Eagles, G., et al. (2020). Deep glacial troughs and stabilizing ridges unveiled beneath the margins of the Antarctic ice sheet. *Nature Geoscience*, *13*(2), 132–137. https://doi.org/10.1038/s41561-019-0510-8

Morlighem, M., Seroussi, H., Larour, E., & Rignot, E. (2013). Inversion of basal friction in Antarctica using exact and incomplete adjoints of a higher-order model. *Journal of Geophysical Research: Earth Surface*, *118*(3), 1746–1753. https://doi.org/10.1002/jgrf.20125

Pelle, T., Greenbaum, J. S., Ehrenfeucht, S., Dow, C. F., & McCormack, F. S. (2024). Subglacial discharge accelerates dynamic retreat of aurora subglacial Basin outlet glaciers, East Antarctica, over the 21st century. *Journal of Geophysical Research: Earth Surface*, *129*(7), e2023JF007513. https://doi.org/10.1029/2023jf007513

Pritchard, H. D., Arthern, R. J., Edwards, L. A., & Vaughan, D. G. (2009). Extensive dynamic thinning on the margins of the Greenland and Antarctic ice sheets. *Nature*, *461*(7266), 971–975. https://doi.org/10.1038/nature08471

19448007, 2026, 15, Downloaded from https://agupubs.onlinelibrary.wiley.com/doi/10.1029/2025GL121190 by Helmholtz-Zentrum Potsdam GFZ, Wiley Online Library on [29/10/2026]. See the Terms and Conditions (https://onlinelibrary.wiley.com/terms-and-conditions) on Wiley Online Library for rules of use; OA articles are governed by the applicable Creative Commons License

Rignot, E., Mouginot, J., & Scheuchl, B. (2017). MEaSUREs InSAR-based Antarctica ice velocity map, version 2 [Dataset]. *Boulder, Colorado USA. NASA National Snow and Ice Data Center Distributed Active Archive Center*. https://doi.org/10.5067/D7GK8F5J8M8R

Schoof, C. (2005). The effect of cavitation on glacier sliding. *Proceedings of the Royal Society A: Mathematical, Physical & Engineering Sciences*, *461*(2055), 609–627. https://doi.org/10.1098/rspa.2004.1350

Sergienko, O. V., & Hulbe, C. L. (2011). Sticky spots' and subglacial lakes under ice streams of the Siple Coast, Antarctica. *Annals of Glaciology*, *52*(58), 18–22. https://doi.org/10.3189/172756411797252176

Seroussi, H., Nowicki, S., Simon, E., Abe-Ouchi, A., Albrecht, T., Brondex, J., et al. (2019). initMIP-Antarctica: An ice sheet model initialization experiment of ISMIP6. *The Cryosphere*, *13*(5), 1441–1471. https://doi.org/10.5194/tc-13-1441-2019

Shreve, R. L. (1972). Movement of water in glaciers. *Journal of Glaciology*, *11*(62), 205–214. https://doi.org/10.3189/S002214300002219X

Siegfried, M. R., Fricker, H. A., Carter, S. P., & Tulaczyk, S. (2016). Episodic ice velocity fluctuations triggered by a subglacial flood in West Antarctica. *Geophysical Research Letters*, *43*(6), 2640–2648. https://doi.org/10.1002/2016GL067758

Sommers, A., Rajaram, H., & Morlighem, M. (2018). SHAKTI: Subglacial hydrology and kinetic, transient interactions v1.0. *Geoscientific Model Development*, *11*(7), 2955–2974. https://doi.org/10.5194/gmd-11-2955-2018

Sommers, A. N., Meyer, C. R., Poinar, K., Mejia, J., Morlighem, M., Rajaram, H., et al. (2024). Velocity of Greenland's Helheim Glacier controlled both by terminus effects and subglacial hydrology with distinct realms of influence. *Geophysical Research Letters*, *51*(15), e2024GL109168. https://doi.org/10.1029/2024gl109168

Stål, T., Reading, A. M., Halpin, J. A., & Whittaker, J. (2020). Antarctic geothermal heat flow model: Aq1 [Dataset]. *PANGAEA*. https://doi.org/10.1594/PANGAEA.924857

Stål, T., Reading, A. M., Halpin, J. A., & Whittaker, J. M. (2021). Antarctic geothermal heat flow model: Aq1. *Geochemistry, Geophysics, Geosystems*, *22*(2), e2020GC009428. https://doi.org/10.1029/2020gc009428

Stearns, L. A., Jezek, K. C., & Van Der Veen, C. (2005). Decadal-scale variations in ice flow along Whillans Ice Stream and its tributaries, West Antarctica. *Journal of Glaciology*, *51*(172), 147–157. https://doi.org/10.3189/172756505781829610

Stearns, L. A., Smith, B. E., & Hamilton, G. S. (2008). Increased flow speed on a large East Antarctic outlet glacier caused by subglacial floods. *Nature Geoscience*, *1*(12), 827–831. https://doi.org/10.1038/ngeo356

van Wessem, J. M., van de Berg, W. J., & van den Broeke, M. R. (2023). Data set: Monthly averaged RACMO2.3p2 variables;Antarctica [Dataset]. *Zenodo*. https://doi.org/10.5281/zenodo.7760491

Warburton, K. L. P., Hewitt, D. R., & Neufeld, J. A. (2023). Shear dilation of subglacial till results in time-dependent sliding laws. *Proceedings of the Royal Society A: Mathematical, Physical and Engineering Sciences*, *479*(2269), 20220536. https://doi.org/10.1098/rspa.2022.0536

Werder, M. A., Hewitt, I. J., Schoof, C. G., & Flowers, G. E. (2013). Modeling channelized and distributed subglacial drainage in two dimensions. *Journal of Geophysical Research: Earth Surface*, *118*(4), 2140–2158. https://doi.org/10.1002/jgrf.20146

Zhao, C., Gladstone, R., Zwinger, T., Gillet-Chaulet, F., Wang, Y., Caillet, J., et al. (2025). Subglacial water amplifies Antarctic contributions to sea-level rise. *Nature Communications*, *16*(1), 3187. https://doi.org/10.1038/s41467-025-58375-4

References From the Supporting Information

Budd, W. F., Keage, P. L., & Blundy, N. A. (1979). Empirical studies of ice sliding. *Journal of Glaciology*, *23*(89), 157–170. https://doi.org/10.3189/S0022143000029804

Dow, C., McCormack, F., Young, D., Greenbaum, J., Roberts, J., & Blankenship, D. (2020). Totten Glacier subglacial hydrology determined from geophysics and modeling. *Earth and Planetary Science Letters*, *531*, 115961. https://doi.org/10.1016/j.epsl.2019.115961

Ehrenfeucht, S., Dow, C., McArthur, K., Morlighem, M., & McCormack, F. S. (2025). Antarctic wide subglacial hydrology modeling. *Geophysical Research Letters*, *52*(1), e2024GL111386. https://doi.org/10.1029/2024GL111386

Glen, J. W., & Perutz, M. F. (1955). The creep of polycrystalline ice. *Proceedings of the Royal Society of London - Series A: Mathematical and Physical Sciences*, *228*(1175), 519–538. https://doi.org/10.1098/rspa.1955.0066

Kamb, B. (1987). Glacier surge mechanism based on linked cavity configuration of the basal water conduit system. *Journal of Geophysical Research*, *92*(B9), 9083–9100. https://doi.org/10.1029/JB092iB09p09083

McArthur, K., McCormack, F. S., & Dow, C. F. (2023). Basal conditions of Denman Glacier from glacier hydrology and ice dynamics modeling. *The Cryosphere*, *17*(11), 4705–4727. https://doi.org/10.5194/tc-17-4705-2023

Mouginot, J., Rignot, E., Scheuchl, B., & Millan, R. (2017). Comprehensive annual ice sheet velocity mapping using Landsat-8, Sentinel-1, and RADARSAT-2 data [Dataset]. *Remote Sensing*, *9*(4), 364. https://doi.org/10.3390/rs9040364

Mouginot, J., Scheuchl, B., & Rignot, E. (2012). Mapping of ice motion in Antarctica using synthetic-aperture radar data. *Remote Sensing*, *4*(9), 2753–2767. https://doi.org/10.3390/rs4092753

Rignot, E., Mouginot, J., & Scheuchl, B. (2011). Ice flow of the Antarctic ice sheet. *Science*, *333*(6048), 1427–1430. https://doi.org/10.1126/science.1208336

Walder, J. S. (1986). Hydraulics of subglacial cavities. *Journal of Glaciology*, *32*(112), 439–445. https://doi.org/10.3189/S0022143000012156

19448007, 2026, 15, Downloaded from https://agupubs.onlinelibrary.wiley.com/doi/10.1029/2025GL121190 by Helmholtz-Zentrum Potsdam GFZ, Wiley Online Library on [29/10/2026]. See the Terms and Conditions (https://onlinelibrary.wiley.com/terms-and-conditions) on Wiley Online Library for rules of use; OA articles are governed by the applicable Creative Commons License